

CHIMIA

CHIMIA 2016, Volume 70
ISSN 0009-4293
www.chimia.ch



SCS
Swiss Chemical
Society

Supplementa to Issue 7-8/2016

SCS Fall Meeting 2016
Oral Presentation Abstracts
Session of Computational
Chemistry

September 15, 2016
University of Zurich, Irchel Campus
<http://scg.ch/fallmeeting/2016>

Swiss Chemical Society
Haus der Akademien
Postfach
3001 Bern
Switzerland
info@scg.ch
www.scg.ch

Industrial Impact of Computational Chemistry and Materials Science

E. Wimmer¹

¹Materials Design s.a.r.l., 92120 Montrouge, France

The combination of powerful theoretical concepts, advanced computational software and today's extraordinary computational capabilities opens unprecedented opportunities for the industrial application of computational chemistry and materials science. This talk will highlight current capabilities in the areas of advanced functional and structural materials as well as molecular systems. In the case of Li-ion batteries, *ab initio* calculations of electrochemical and structural properties have been successful in identifying candidates for low-strain cathode materials [1]. Simulations of Li diffusion in the solid state electrolyte $\text{Li}_{10}\text{GeP}_2\text{S}_{12}$ (LGPS) on crystalline vs. polycrystalline and amorphous structures have revealed the effect of structural changes on ion conductivity. Hydrogen embrittlement of metal alloys has its origins in chemical interactions, diffusion, and formation of metal hydrides. Detailed computational investigations of these phenomena have led to deeper insight as well as quantitative materials property data, which form the basis for systematic improvements of structural materials [2]. The systematic prediction of thermodynamic and thermochemical properties of molecular systems and fluids illustrates another aspect of the value of theoretical and computational approaches [3]. All of the above applications are facilitated by advanced capabilities implemented in the MedeA[®] software [4]. An assessment of the current state of the art and the challenges for future research will conclude this talk.

[1] F. Rosciano, M. Christensen, V. Eyert A. Mavromaras, and E. Wimmer, *International Patent Publication*. **2014**, WO2014191018 A1.

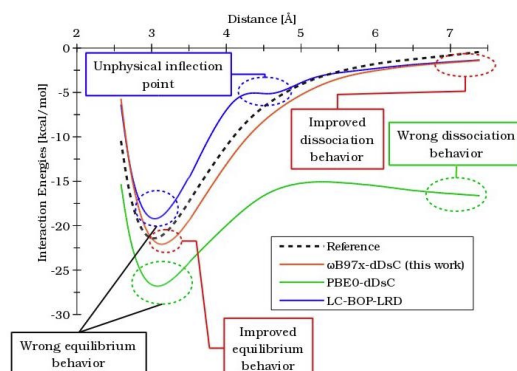
[2] M. Christensen, W. Wolf, C. Freeman, E. Wimmer, R. B. Adamson, L. Hallstadius, P. E. Cantonwine, and E. V. Mader, *J. Phys.: Condens. Matter*. **2014**, 27, 025402.

[3] X. Rozanska, J. J. P. Stewart, P. Ungerer, B. Leblanc, C. Freeman, P. Saxe, and E. Wimmer, *J. Chem. Eng. Data*. **2014**, 59, 3136.

[4] MedeA[®] Software Environment, *Materials Design, Inc.*, **1998-2016**;
<http://www.materialsdesign.com>

Balancing London dispersion and the delocalization error with DFT functionalsA. Fabrizio¹, R. Petraglia¹, C. Corminboeuf^{1*}¹Laboratory for Computational Molecular Design, ISIC, EPFL, Lausanne, Switzerland

π -dimer radical cations are the simplest model systems for the computational description of charge carriers in organic electronic materials. In 2012, Steinmann and Corminboeuf introduced a benchmark database of π -dimer radical cations (Orel26rad) and demonstrated that none of the most widely-used dispersion corrected density functionals are able to achieve accurate binding energies together with a correct dissociative behavior [1]. In the same work the authors concluded that the challenging nature of these compounds originates from the inability of the functionals to properly account for London dispersion interactions and simultaneously avoid spurious charge delocalization [1]. Here, we propose the development and the optimization of a new dispersion corrected, range-separated hybrid density functional (ω B97x-dDsC), specifically conceived to achieve a balanced description of both delocalization error and long-range dispersion interactions. In particular, inspired by the overall satisfactory performance of ω B97x-D [2] on the Orel26rad dataset, we jointly-fitted the parameters that tune the damping function of the dDsC dispersion correction with the ones that regulate the core of the functional (ω B97x). ω B97x-dDsC was found able to provide highly accurate binding energies for the π -dimer radical cations not only around the equilibrium structure, but also in the asymptotic region towards the dissociation limit of the dimers. Our functional shows no significant deterioration of the description of other chemical properties when compared to existing functionals of the same family (e.g. ω B97x-D).

[1] S.N. Steinmann and C. Corminboeuf, *J. Chem. Theory Comput.* 8, 4305 (2012)[2] J.D. Chai and M. Head-Gordon, *Phys. Chem. Chem. Phys.* 10, 6615 (2008)

A fast scheme for approximated Fock exchange potentials in plane wave implementations of Kohn-Sham Density Functional Theory

M. Bircher¹, S. Meloni¹, U. Röthlisberger^{1*}

¹EPF Lausanne

With the considerable increase in sampling efficiency of Kohn-Sham density functional theory (KS-DFT) based first-principles molecular dynamics, the availability of more accurate but cost-effective exchange-correlation functionals has become of central importance to the field.

Plane wave/pseudo potential based first-principles molecular dynamics simulations are typically limited to the use of generalised-gradient approximation (GGA) exchange-correlation functionals. While hybrid functionals, which combine a certain amount of Hartree-Fock exchange with a (semi-)local KS-formalisms, are more accurate for a wide range of applications, the computational burden associated with the evaluation of the exact exchange integrals substantially limits the accessible time scales.

Here, we present a novel multi-grid scheme for the evaluation of Fock exchange integrals in a plane wave basis based on the combined direct/momentum space implementation used in the CPMD code, where orbital pair products are computed in real space and their corresponding Coulomb potential is obtained in momentum space. Direct and momentum space representations are linked via fast Fourier transforms (FFTs).

In the proposed scheme, high frequency components of the momentum space representation of orbital pair products are mapped onto analytic or numerical atom-centred auxiliary functions. These functions have a (pseudo) compact domain in direct space, which allows for an efficient calculation of their overlap with orbital pair products. The residual obtained from subtracting overlap-weighted auxiliary functions from the orbital pairs obtained on the standard FFT grid is mapped on a coarse, commensurate grid, and the associated Coulomb potential is calculated using the standard algorithm, but with a considerably lower plane wave cutoff. The Coulomb potential associated to the auxiliary functions is precomputed at the beginning of every SCF cycle on the full FFT grid. The residual Coulomb potential is interpolated onto the standard grid in direct space, and then added to the precomputed auxiliary Coulomb potential and, subsequently, the forces acting on the plane wave coefficients are determined via a further FFT.

This scheme allows for two Fourier transforms, which are usually calculated at the full density cutoff, to be carried out with a cutoff value typically 16-fold lower than the full density cutoff, corresponding to a four-fold increased grid spacing during the transforms of the residual. We will present speed ups compared to the standard algorithm and discuss issues linked to the choice of optimal auxiliary basis functions that guarantee sufficient smoothness of the residual function.

Quantitative Reaction Energies from an Automated Multi-Configurational Approach

C. Stein¹, V. von Burg¹, M. Reiher^{1*}

¹ETH Zürich

Quantum-chemical multi-configurational methods yield qualitatively correct wave functions for molecules with close-lying frontier orbitals. This class of methods, however, requires the manual selection of a subset of so-called active orbitals within which all possible configurations are considered. A poor choice of this subset leads to the exclusion of important configurations and therefore to wrong results. Quantitative data further requires perturbation theory to consider the dynamic electron correlation which makes the active orbital selection even more delicate. Currently, these active orbitals are selected based on empirical rules[1] or natural orbital occupation numbers of a precedent calculation.[2]

Here, we propose selection criteria that additionally take entropy based orbital entanglement measures into account.[3] We therefore exploit the ability of the density matrix renormalization group (DMRG) algorithm to approximate the entanglement information of a large number of active orbitals. The orbital selection protocol based on these criteria is fully automated and applied for the calculation of the heterolytic dissociation energy of four metallocenes $M(\text{Cp})_2$, with $M = \text{V}, \text{Mn}, \text{Fe}$ and Ni .[4]

The final energies are obtained from complete active space self-consistent field calculations with second-order perturbation theory. We compare the results of these multi-configurational calculations with those of a highly accurate coupled-cluster approach.

[1] V. Veryazov, P.-Å. Malmqvist, B. O. Roos, *Int. J. Quantum Chem.*, **2011**, 111, 3329-3338.

[2] S. Keller, K. Boguslawski, T. Janowski, M. Reiher, P. Pulay, *J. Chem. Phys.*, **2015**, 142, 244104.

[3] C. J. Stein, M. Reiher, *J. Chem. Theory Comput.*, **2016**, 12, 1760.

[4] C. J. Stein, V. von Burg, M. Reiher, *to be submitted*.

FDE-ADC: Multiscale density embedding with an accurate wavefunction method.A. Zech¹, S. Prager², T. A. Wesolowski^{1*}, A. Dreuw^{2*}¹University of Geneva, ²University of Heidelberg

In the presence of an environment, excitation energies, properties and sometimes even reactivity of the target molecule may change drastically. Thus, including environmental effects into quantum chemical calculations either by implicit or explicit models is necessary for an adequate description of these systems. Frozen-Density Embedding Theory (FDET) [1;2] provides a formal framework in which the whole system is described by means of two independent quantities: the embedded wavefunction (interacting or not) and the density associated with the environment. The FDET approach can conveniently be combined with perturbative wavefunction methods, e.g. the Algebraic Diagrammatic Construction (ADC) scheme for the polarization propagator.

We present the new multiscale variant FDE-ADC [3] as a combination of FDET and ADC. The current implementation of FDE-ADC uses the Linearized FDET formalism [4], which in comparison to FDET, is significantly less expensive computationally and more importantly leads to self-consistency between the energy and embedding potential preserving simultaneously the orthogonality of the embedded wavefunctions for each electronic state.

Three molecular model systems were studied using two different FDE-ADC techniques in which the environment consisted of up to five water molecules. The molecular test systems were chosen to investigate molecule - environment interactions of varying strength from dispersion interaction up to multiple hydrogen bonds. The overall difference between the supermolecular ADC calculations and the FDE-ADC calculations in excitation energies is lower than 0.09 eV (max) and 0.032 eV in average. Also oscillator strengths are reproduced in good agreement with the supermolecular calculation. Initial results show that the FDE-ADC method is a promising approach for considering environmental effects on electronically excited states.

[1] T. A. Wesolowski, A. Warshel, *J. Phys. Chem.*, **1993**, 97, 8050–8053.

[2] T. A. Wesolowski, *Phys. Rev. A*, **2008**, 77, 012504.

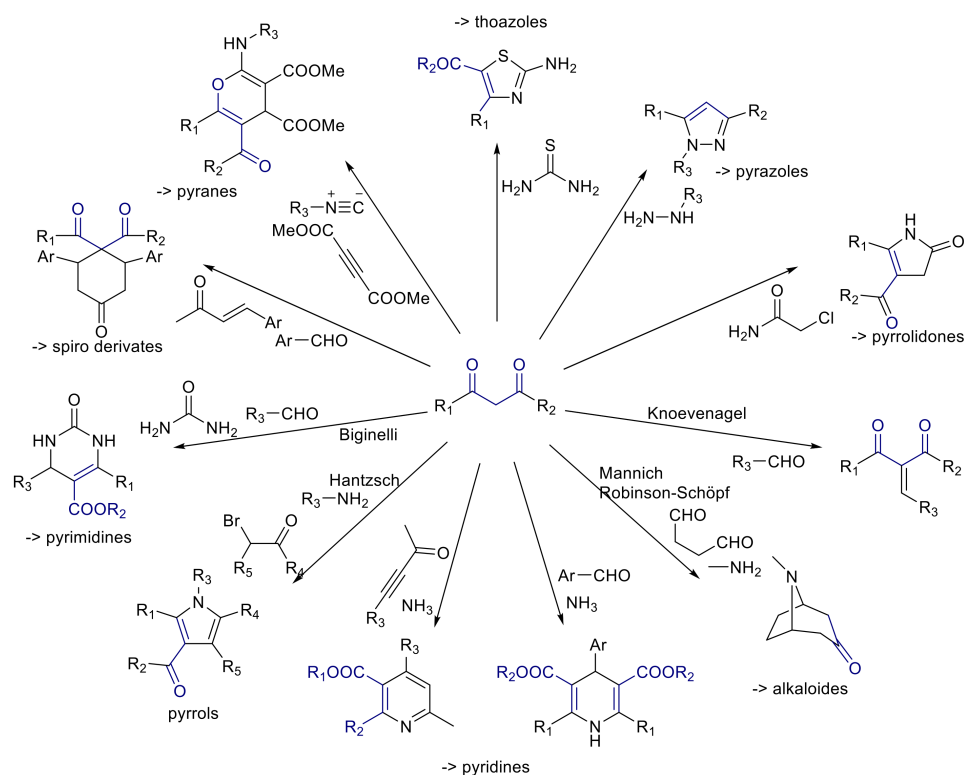
[3] S. Prager, A. Zech, F. Aquilante, A. Dreuw, T. A. Wesolowski, **2016** (submitted to *J. Chem. Phys.*).

[4] A. Zech, F. Aquilante, T. A. Wesolowski, *J. Chem. Phys.*, **2015**, 143, 164106.

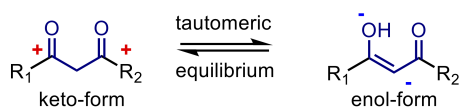
Industrial modeling aspects of 1,3-dicarbonyl compounds

C. Taeschler¹¹Lonza AG

1,3-Dicarbonyl compounds are an important class of intermediates used in the pharma and agrochemical industry as well as in material sciences. As a manufacturer of over 100 intermediates of this class, LONZA Ltd provides a large assortment of these compounds to serve numerous industrial applications [1].



In order to provide a state-of-the-art service, a fundamental knowledge of this class of compounds is essential, which is obtained by measurements and increasingly, by molecular modeling.



In this talk, some aspects of the properties and the insights gained by *in silico* experiments of 1,3-dicarbonyl compounds are discussed.

[1] a) C. Taeschler, in *Kirk-Othmer Encyclopedia of Chemical Technology*, John Wiley Sons, Inc., **2009**. b) R. Miller, C. Abaecherli, A. Said and B. Jackson, in *Ullmann's Encyclopedia of Industrial Chemistry*, Wiley-VCH Verlag GmbH Co. KGaA, **2000**. c) Benetti, S.; Romagnoli, R.; De Risi, C.; Spalluto, G.; Zanirato, V. Mastering .beta.-Keto Esters. *Chemical Reviews* **1995**, *95*, 1065-1114. d) Duque, M. d. M. S.; Allais, C.; Isambert, N.; Constantieux, T.; Rodriguez, J. β -Diketo building blocks for MCRs-based syntheses of heterocycles. *Top. Heterocycl. Chem.* **2010**, *23*, 227-277.

Is oxide hydrogenation equivalent to reduction? Fundamental differences between TiO_2 and Al_2O_3 from DFT

C. Spreatico¹, W. Karim², A. Kleibert³, J. Gobrecht³, Y. Ekinici³, J. A. van Bokhoven², J. VandeVondele^{1*}

¹ETH Zurich, ²ETH Zurich/PSI Villigen, ³Paul Scherrer Institute, Villigen

TiO_2 and Al_2O_3 are universally employed supports in heterogeneous catalysis[1]. Depending on the support, however, there are sensible performance differences, the origin of which, at present, is poorly understood. In addition, reduced oxides, in particular TiO_2 , hold great promise as a support for efficient photocatalytic devices[2]. Hydrogen spillover from a supported metal cluster is widely employed in hydrogenation reactions and could also be adopted as a convenient way to introduce "engineered disorder" in the titania structure[3], thus enhancing its light adsorption properties and electrical conductivity[4].

Here the interface reactivity and electronic structure of hydrogen-reduced TiO_2 and Al_2O_3 are investigated with GGA and hybrid DFT methods, including ab initio thermodynamics and Nudged Elastic Band (NEB) calculations. The calculations results are also compared and integrated to data obtained from a novel approach based on top-down nanofabrication and spatially-resolved in-situ X-ray absorption spectro-microscopy.

We demonstrate that, upon H_2 adsorption, two protons are bound to surface oxide anions, while two electrons are transferred to the oxide, creating electronic trap sites (formal Ti(III) centers) that strongly interact with the surface protons. Even though surface protons are highly mobile on the titania interface (particularly in presence of coadsorbed water molecules), the same can not be said for the Ti(III) centers, and thus the combined migration rate (e^-/H^+) of adsorbed H atoms is slower. As demonstrated in a previous study [5] defect concentration effects are also relevant: stronger H-oxide interaction is obtained at lower concentrations, as modelled with a realistic titania slab (~ 1000 atoms) and hybrid functionals.

The case of gamma- Al_2O_3 is instead quite different: instead of homolytic H_2 splitting and oxide reduction, on Al_2O_3 the hydrogen molecule split in a heterolytic manner, with formation of a proton, bound to a surface oxide anion, and of an hydride moiety, bound to particularly reactive surface Al tricoordinated ($\text{Al}3\text{c}$) site. On the other hand, the electronic structure of the oxide is only marginally altered, without formation of defect states in the oxide band gap. In addition, the mobility of the hydride moiety is limited, in particular in presence of coadsorbed water molecules. Hydrogen spillover from a Pt cluster to TiO_2 has also been modelled, demonstrating that the spillover rate depends on the cluster hydrogen load and on the thickness of the oxide acceptor layer.

To conclude, even if hydrogen molecules can exothermically adsorb on both TiO_2 and Al_2O_3 surfaces, only in the first case oxide reduction, with formation of polaronic states, is achieved, while for alumina reducing species are confined at the interface, and demonstrate a lower mobility.

References

- [1] A. Chen and P. Holt-Hindle, Chem. Rev., 110(6):3767–3804, JUN 2010.
- [2] M. Ni, M. K. H. Leung, D.Y. C. Leung, and K. Sumathy, Ren. Sust. En. Rev., 11(3):401–425, 2007.
- [3] X. Chen, L. Liu, P. Y. Yu, and S.S. Mao., Science, 331(6018):746–750, 2011.
- [4] J. Nowotny, T. Bak, M.K. Nowotny, and L.R. Sheppard, J. Phys. Chem. C, 112(14):5275–5300, 2008.
- [5] C. Spreatico and J. VandeVondele., Phys. Chem. Chem. Phys., 16:26144–26152, 2014.

Interatomic many-body representation improves molecular machine learning models

B. Huang¹, O. Lilienfeld^{1*}¹Institute of Physical Chemistry and National Center for Computational Design and Discovery of Novel Materials (MARVEL), Department of Chemistry, University of Basel

We introduce an improved molecular representation based on expanding the total energy of the system in interatomic many-body interaction potentials (MBP) including bags of atoms (BoA), and bags of pairs (BoP), triplets (BoT), and quadruplets (BoQ) of atoms. Specific values correspond to the Universal Force Field^[1] or other well established potentials. When considering only BoA+BoP, with BoA and BoP being the respective diagonal and off-diagonal elements in Coulomb matrix (CM), the resulting descriptor performs as well as BoB^[2]. Inclusion of BoT and BoQ systematically improves the off-set as well as the learning rate. Out-of-sample prediction errors for G4MP2 quality properties of thousands of constitutional isomers decay systematically, reaching unprecedented chemical accuracy (~ 1 kcal/mol) for machine learning models trained on 5k molecules.

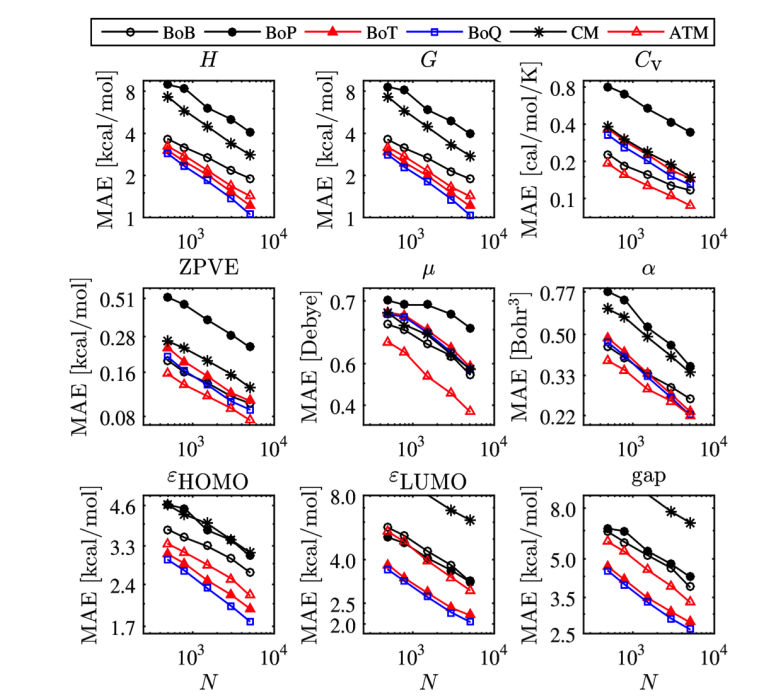


Figure 1. Single kernel^[3] learning curves for H : enthalpy, G : free energy, C_v : heat capacity, ZPVE: zero point vibrational energy, μ : dipole moment, α : polarizability, ϵ_{HOMO} : HOMO energy, ϵ_{LUMO} : LUMO energy and HOMO-LUMO gap. Mean absolute errors are shown as a function of training set size for out of sample property predictions of the remainder of 6095 constitutional isomers of $\text{C}_7\text{H}_{10}\text{O}_2$ ^[4], drawn from GDB-17^[5] database. MAEs are shown for 6 different representations: CM^[2], BoB^[2], BoB+ATM (Axilrod-Teller-Muto vdW potential)^[6], BoP, BoT and BoQ.

*anatole.vonlilienfeld@unibas.ch

[1] A. K. Rappe et al., *J. Am. Chem. Soc.*(1992)[2] M. Rupp et al., *Phys. Rev. Lett.* (2012); K. Hansen et al., *J. Phys. Chem. Lett.*(2015)[3] R. Ramakrishnan and O. A. von Lilienfeld, *CHIMIA* (2015)[4] R. Ramakrishnan et al., *Sci. Data*, **1** (2014), 140022.[5] T. Fink et al., *Angew. Chem. Int. Ed.* (2005), L. Ruddigkeit et al., *J. Chem. Inf. Model.* (2012)[6] B. M. Axilrod and E. Teller, *J. Chem. Phys.*(1943); Y. Muto, *J. Phys. Math. Soc. Japan.* (1943)

Reactive Molecular Dynamics and Infrared Spectra of Double Proton Transfers with Coupling Effects

Z.-H. Xu¹, K. Mackeprang², Z. Maroun², H. Kjaergaard², M. Meuwly^{1*}

¹University of Basel, ²University of Copenhagen

For simulating double proton transfer (DPT) reactions of formic acid in dimeric forms, the previously developed Molecular Mechanics with Proton Transfer (MMPT) method has been further improved by introducing coupling effects which accurately provides an energetic description for the DPT reactions in atomistic simulations. From the experiments, the infrared spectra of formic acid dimer (FAD) and its deuterated isotopologues have been reported at the gas phase with low pressures by using spectral subtraction. And the broad OH-stretch spectral signatures (2600~3400 cm⁻¹) agree well with previously recorded spectra. In order to align between the simulated and experimentally resultant spectral features in the proton transfer region, potential morphing was also carried out with the electronic structure calculations at the B3LYP and MP2 levels respectively. In this work, a barrier for DPT in FAD has been estimated as 5~7 kcal/mol which compares with a barrier of 7.9 kcal/mol from CCSD(T)/aug-cc-pVTZ calculations. Such a combination of experimental and computational techniques helps the barrier estimations for intramolecular proton transfer reactions, of which the reaction kinetics is not easy to be measured directly in experiments. And the further improvement of energetics of these reactive systems is also feasible and expected.

[1] K. Mackeprang, Z.-H. Xu, Z. Maroun, M. Meuwly, and H. G. Kjaergaard. Spectroscopy and Dynamics of Double Proton Transfer in Formic Acid Dimer. (2016, submitted)

[2] S. Lammers, S. Lutz and M. Meuwly, J. Comput. Chem, 2008, 29, 1048-1063.

[3] Y. Yang and M. Meuwly, J. Chem. Phys., 2010, 133, 064503

[4] D. L. Howard, H. G. Kjaergaard, J. Huang and M. Meuwly, J. Phys. Chem. A, 2015, 119, 7980-7990

On the ultrashort pulse approximation for the interaction of molecule with pulsed laser fields: Generalization of the Franck-Condon principleA. Patoz¹, J. Vanicek^{1*}¹EPF Lausanne

We explore several possible definitions of an “ultrashort laser pulse” and derive approximate geometric integrators for the nonadiabatic molecular quantum dynamics induced by interaction with such pulses. For a particular definition combined with the time-dependent perturbation theory, we are able to derive an analytical expression for the quantum evolution operator, which enormously speeds up numerical calculations. Our analytical formula can be understood as the generalization of the Franck-Condon principle to ultrashort pulses of arbitrary shapes. Finally, we show that in the limit of the pulse width going to zero, we recover the widely used and surprisingly accurate δ -pulse approximation.

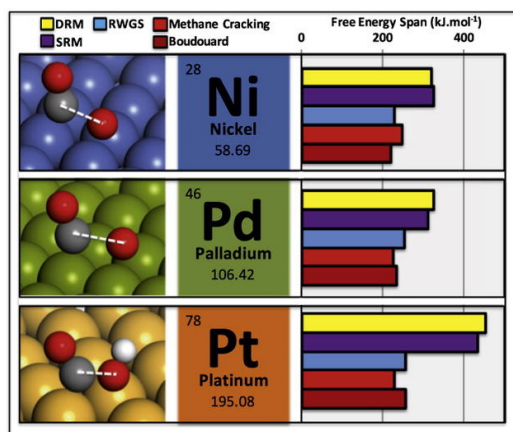
The performance of the introduced approximations is illustrated using the three-state three-dimensional vibronic coupling model of pyrazine in which it is essential to go beyond the δ -pulse limit in order to describe the dynamics correctly.

Dry Reforming and Competitive Reactions on Ni, Pd and Pt metal Surfaces from DFT Calculations and Microkinetic Modeling Simulations

A. Comas-Vives¹, L. Foppa¹, M. Silaghi¹, K. Larmier^{2*}

¹ETH Zürich, ²ETH Zurich

Dry (CO₂) reforming of methane converts CH₄ and CO₂ to syngas (CO and H₂), however, the high temperatures needed for the reaction and the occurrence of competitive reactions (especially coke formation) are factors that hinder their development. Herein, we provide a comparative mechanistic study of dry reforming reaction network at 700 °C on group 10 (Ni, Pd, Pt) (111) metal surfaces using periodic *ab initio* calculations and microkinetic modeling simulations.¹ While the CH₄ dissociation energy barrier is found to be metal independent, our calculations show that CO₂ dissociation is more energy-demanding following the trend Ni < Pd < Pt. As a consequence, the activation of CO₂ via C-O bond cleavage is less energy demanding than the CH₄ activation in the case of Ni, but not for Pd and Pt surfaces. All three metals share the same preferred dry reforming route via HCO* intermediate, but the overall energy span increases in the order Ni ≈ Pd ≪ Pt. Nevertheless, our microkinetic simulations suggest that only Ni (111) surface is significantly active in dry reforming, which is related to the balance between energy barriers of CH₄ and CO₂ activation processes. Another differences among these metals concern the carbon-carbon bond formation during coke production, which becomes less favorable from Ni to Pt, and the preferred reaction path for the reverse water gas shift reaction: via direct (Ni and Pd) or hydrogen-assisted (Pt) CO₂ dissociation. By comparing the reactivity of Ni, Pd and Pt surfaces, we highlight the important catalyst features needed for a good dry reforming performance in order to envisage more active and selective catalysts for this reaction.



[1] Lucas Foppa, Marius-Christian Silaghi, Kim Larmier, Aleix Comas-Vives, *Journal of Catalysis*, **2016**, in press.